

# M.C. Studies of GlueX Solenoidal Field I

David Lawrence

August 2009

## 1 Introduction

This document outlines a couple of brief simulation studies to gauge the impact of uncertainties in the magnetic field map of the GlueX superconducting solenoidal magnet. Two main studies were done, both of which simulated the detector response with *hdgeant* using one field map and then reconstructing the events using a different field map. The first study applied algorithmic deformations to the field in a systematic albeit non-physical way. The second study used maps generated with the POISSON/Superfish package with coils shifted small amounts in  $z$ . Both studies indicated that material effects (multiple scattering and energy loss) in the detector dominated detector resolution and systematics. Changes to the field due to coil position uncertainty will have a relatively small effect providing no motivation for detailed mapping of the magnet.

## 2 Spoiled Map Study

A "spoiled" map option has been added to the GlueX simulation/reconstruction software that can be specified instead of one of the nominal 2-D maps that are available. When this option is chosen, it uses the nominal map and tweaks the magnitude based on the  $r$ ,  $\theta$ , and  $\phi$  coordinates of the requested point before the value is passed on to the requester. Because only the magnitude is modified, the map is non-physical, but should be close enough to suffice for the present purpose.

Figures 1, 2, and 3 show the a comparison of the spoiled map to the nominal map generated by ANSYS. Studies were done reconstructing with maps spoiled by both 1% and 5%.

Figure 4 shows the tracking efficiency for fully reconstructed, single  $\pi^+$  tracks in the forward (FDC + transition) region. The plots show that the overall tracking efficiency is not affected by the spoiled field, even when spoiled at the 5% level.

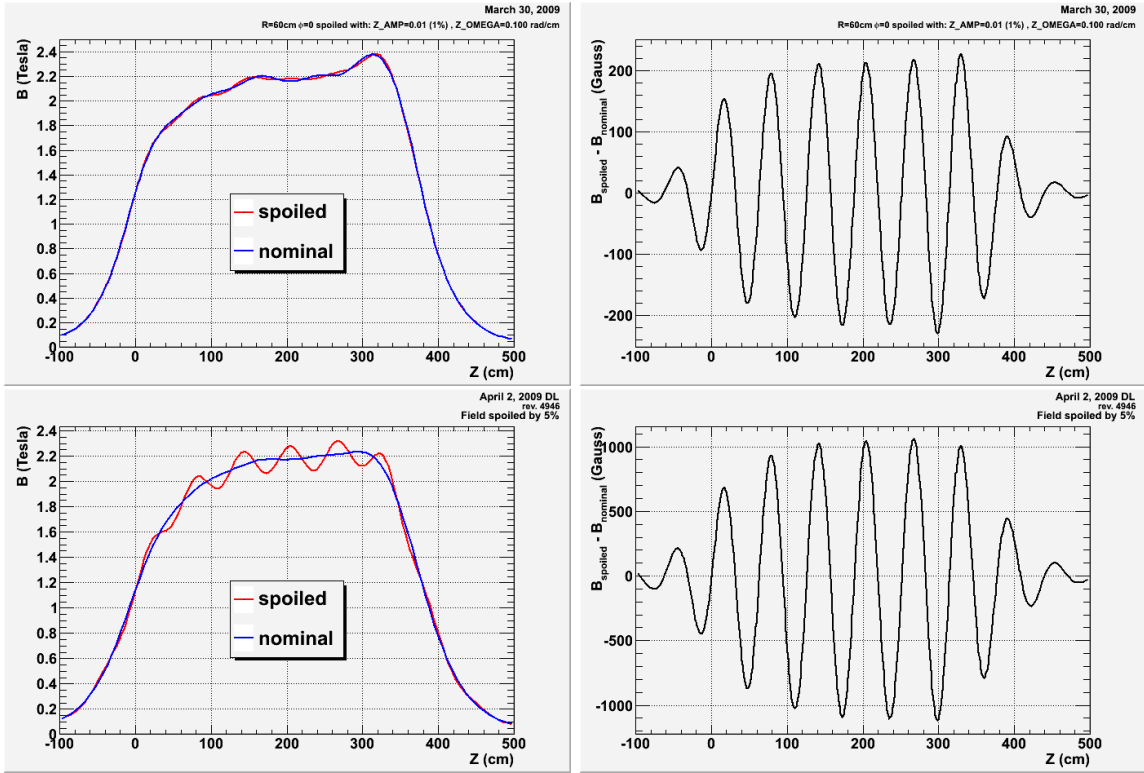


Figure 1: Comparison of B-Field maps spoiled algorithmically to the nominal ANSYS map. The plots on the left are of the field magnitude and the plots on the right are of the difference in magnitude between the spoiled and nominal maps. The plots on the top are for when the field is spoiled by 1% and the plots on the bottom are for when the field is spoiled by 5%. Here, the maps are spoiled only as a function  $r$ .

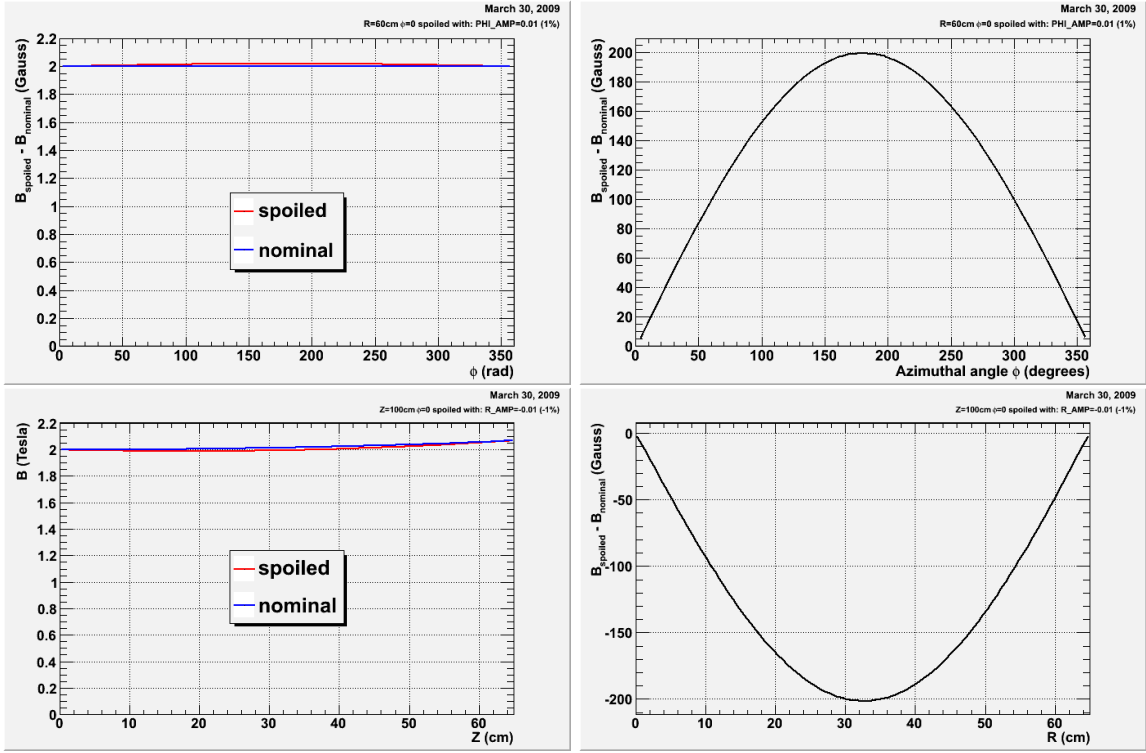


Figure 2: Similar to figure 1 but as a function of the  $\phi$  angle (top) and radial distance (bottom).

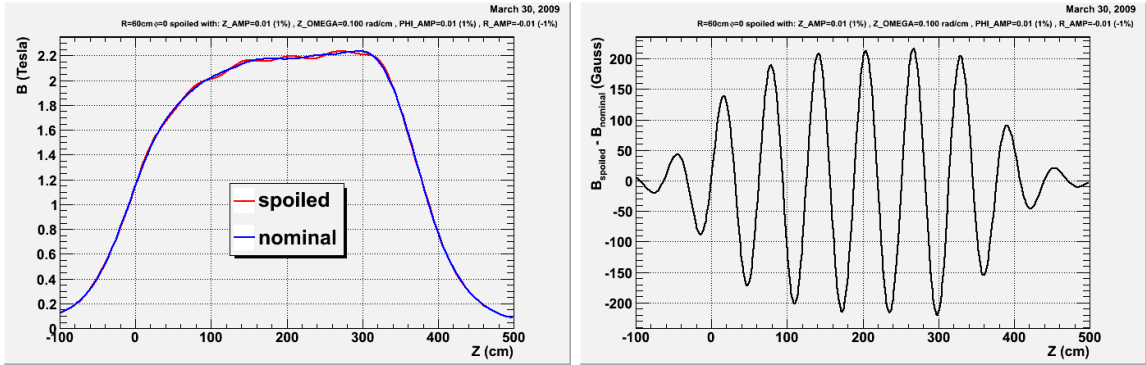


Figure 3: Similar to figure 1, but with spoiling in all 3 cylindrical coordinates ( $r$ ,  $\phi$ , and  $z$ ). The field is spoiled by a maximum of 1% for each dimension.

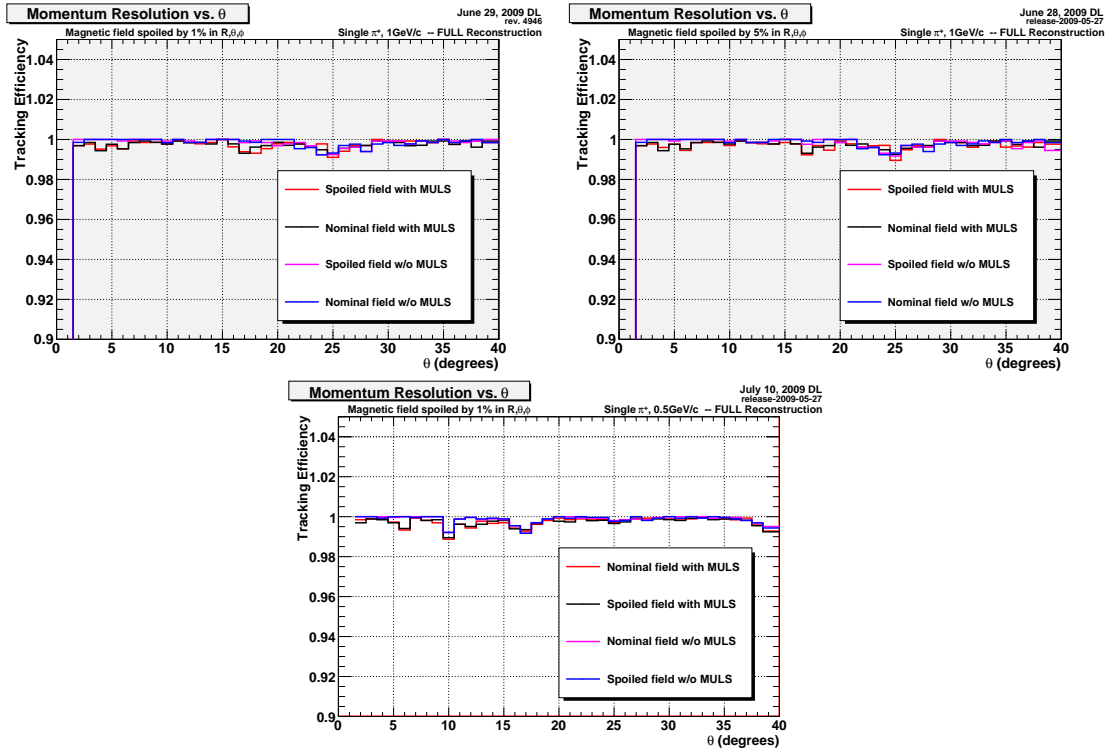


Figure 4: Tracking efficiency in the forward (FDC) region as a function of  $\theta$  for when the field used for reconstruction was spoiled algorithmically from the nominal ANSYS map used during the simulation. The top two plots are for 1GeV/c  $\pi^+$  tracks when the field was spoiled by 1% (left) and 5% (right). The bottom plot is for 500MeV/c  $\pi^+$  tracks when the field was spoiled by 1%.

Figure 5 shows the tracking efficiency for fully reconstructed, single  $\pi^+$  tracks in the barrel (CDC) region. The plots show that the overall tracking efficiency is not affected by the spoiled field, even when spoiled at the 5% level. Note that in the plots it appears that when tracks are reconstructed with a 5% spoiled field that the tracking efficiency with multiple scattering actually improves. This is just due to the cut on the reduced  $\chi^2$  being raised for the 5% case. The important feature of both graphs is that the efficiencies of the spoiled and nominal maps are essentially the same in both cases.

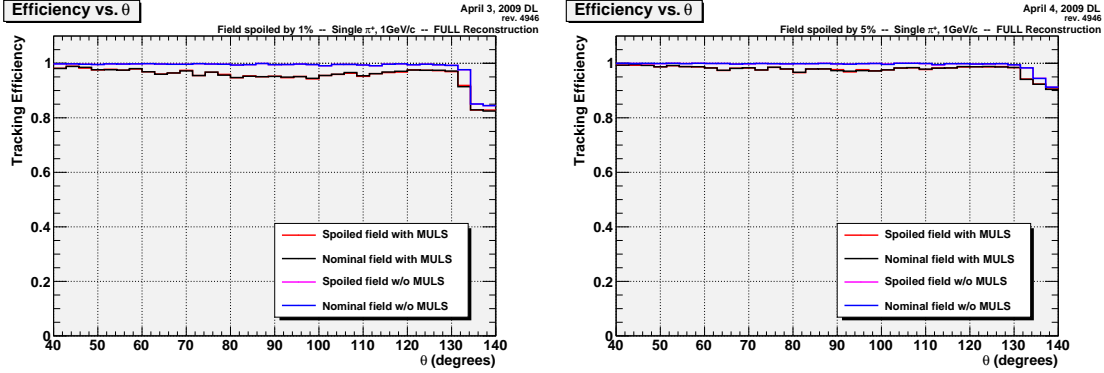


Figure 5: Tracking efficiency in the barrel (CDC) region as a function of  $\theta$  for when the field used for reconstruction was spoiled algorithmically from the nominal ANSYS map used during the simulation. The two plots are for 1GeV/c  $\pi^+$  tracks when the field was spoiled by 1% (left) and 5% (right).

Figure 6 shows total momentum resolution plots of both the systematic and statistical errors for single  $\pi^+$  tracks in the forward (FDC) region. The plots indicate that there is no significant effect when the field is spoiled by 1%. The 5% spoiled field case represented by the plots on the bottom row indicate a noticeable effect on both the systematic error and resolution on the momentum. Specifically, there is an  $\sim 1.5\%$  increase in both the systematic and statistical error in the  $10^\circ$ - $20^\circ$  range for 1GeV/c  $\pi^+$  tracks when reconstructed with a 5% spoiled field.

Figure 7 shows total momentum resolution plots of both the systematic and statistical errors for single  $\pi^+$  tracks in the barrel (CDC) region. The plots indicate that when spoiling the field by 1% the systematic error in the CDC region reaches as high as 1%. The systematic error, however seems unaffected. For the case of a 5% spoiled field, the effect is more pronounced rising as high as 3% systematic and 1.6% systematic. Larger systematic effects are observed in the backwards angles ( $\geq 100^\circ$ ) but these angles are sparsely populated by the physics of interest and perhaps poses less of a concern.

there is no significant effect when the field is spoiled by 1%. The 5% spoiled field case represented by the plots on the bottom row indicate a noticeable effect on both the systematic error and resolution on the momentum.

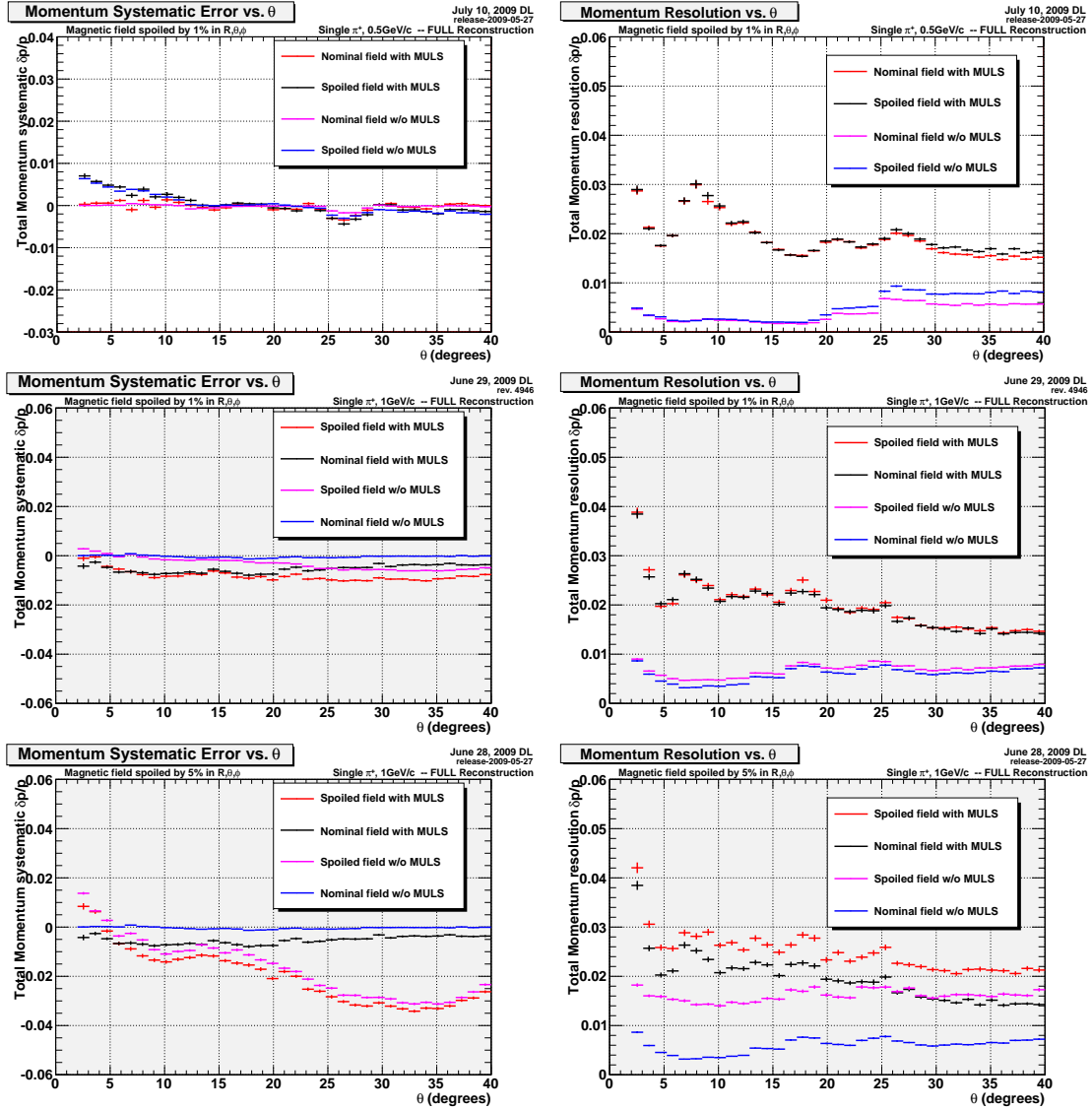


Figure 6: Systematic (left) and statistical (right) uncertainty in reconstructed tracks in the forward (FDC) region as a function of  $\theta$ . The top row is for 500MeV/c  $\pi^+$  tracks with a field spoiled by 1%. The middle row is 1GeV/c  $\pi^+$  with a 1% spoiled field. The bottom row is for 1 GeV/c  $\pi^+$  with a 5% spoiled field.

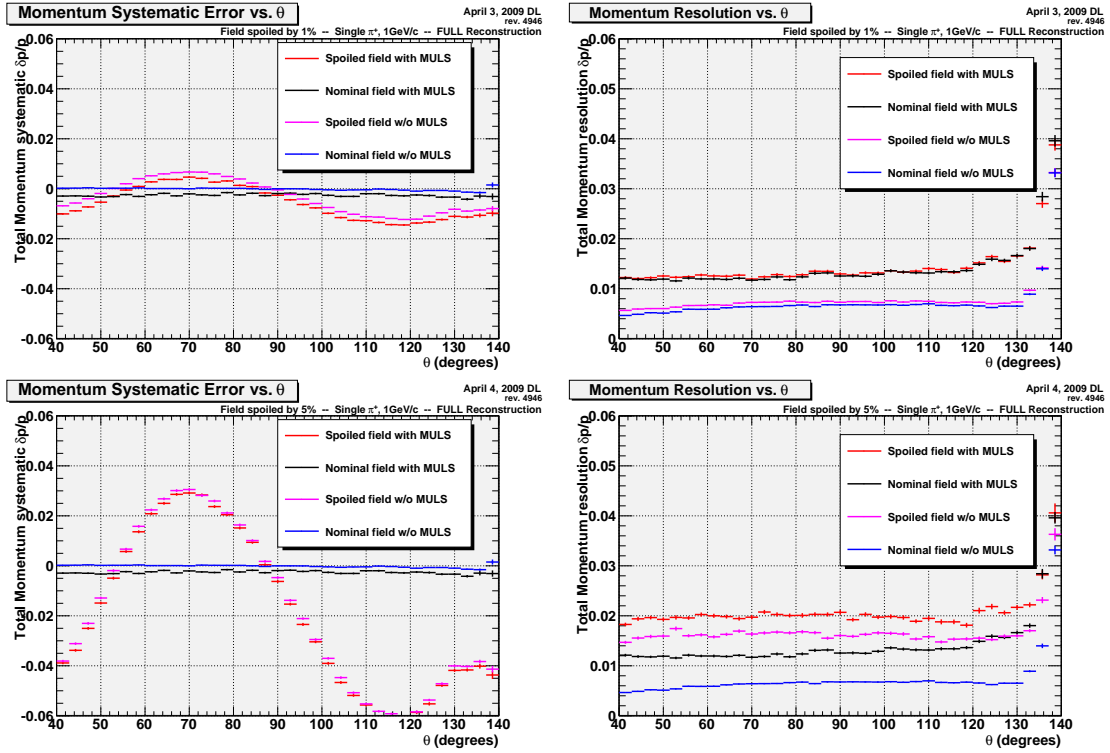


Figure 7: Systematic (left) and statistical (right) uncertainty in reconstructed tracks in the barrel (CDC) region as a function of  $\theta$ . The top row is 1 GeV/c  $\pi^+$  with a 1% spoiled field. The bottom row is for 1 GeV/c  $\pi^+$  with a 5% spoiled field.

Table 1: Field maps used in the current study.

Map	Description
20090312-2	ANSYS map currently used as default in simulation/reconstruction
poisson_20090813_01	Eugene’s original poisson map (current is backwards)
poisson_20090814_01	same as poisson_20090813_01 but with current flipped
poisson_20090814_02	same as poisson_20090814_01 but with current reduced by 1% in all coils
poisson_20090826_01	same as poisson_20090814_01 but with double the mesh point density in both dimensions
poisson_20090827_01	same as poisson_20090814_01 but with coils 1,2,3,4 shifted z=-1.0,-0.5,+0.5,+1.0cm respectively
poisson_20090827_02	same as poisson_20090814_01 but with coils 1,2,3,4 shifted z=-2.0,-1.0,+1.0,+2.0cm respectively
poisson_20090827_03	same as poisson_20090814_01 but with coils 1,2,3,4 shifted z=-4.0,-2.0,+2.0,+4.0cm respectively
poisson_20090827_04	same as poisson_20090814_01 but with coils 1,2,3,4 shifted z=+2.0,+1.0, 0.0, 0.0cm respectively

### 3 Field Map Calculations

A second study was done using more realistic maps generated with coil positions either shifted in z from the nominal, or with the current lowered by 1% from the nominal (1500A). Table 1 lists the field maps used in this set of studies and referenced throughout the rest of this document.

#### 3.1 Comparison of Maps

Figures 8 and 9 show graphically the fields of the 4 maps generated with coil positions shifted relative to the nominal (not shown). By eye, one can see no variation in the region of the tracking chambers (R;55cm).

Figures 10, 11, and 12 show plots comparing a field map generated by the POISSON/Superfish program suite to the our nominal map generated by ANSYS. POISSON was used to generated all of the shifted geometries because it was more accessible than ANSYS. Figure 10 shows the two programs generate maps with the same general features. Figure 11 shows the difference between the ANSYS and POISSON generated maps in both magnitude and angle of the magnetic field. The two maps appear consistent in the region of the tracking chambers as indicated on the plot with the exception of the region nearest to the beamline at R;6cm. It should be noted that the ANSYS map has a geometry that cuts out the 1cm “tip of the wedge” closest to the beamline. This is due to ANYS using a 1° wedge of a full 3-D model to calculate the field and the 1cm cutoff allowed use of a much simpler mesh method.

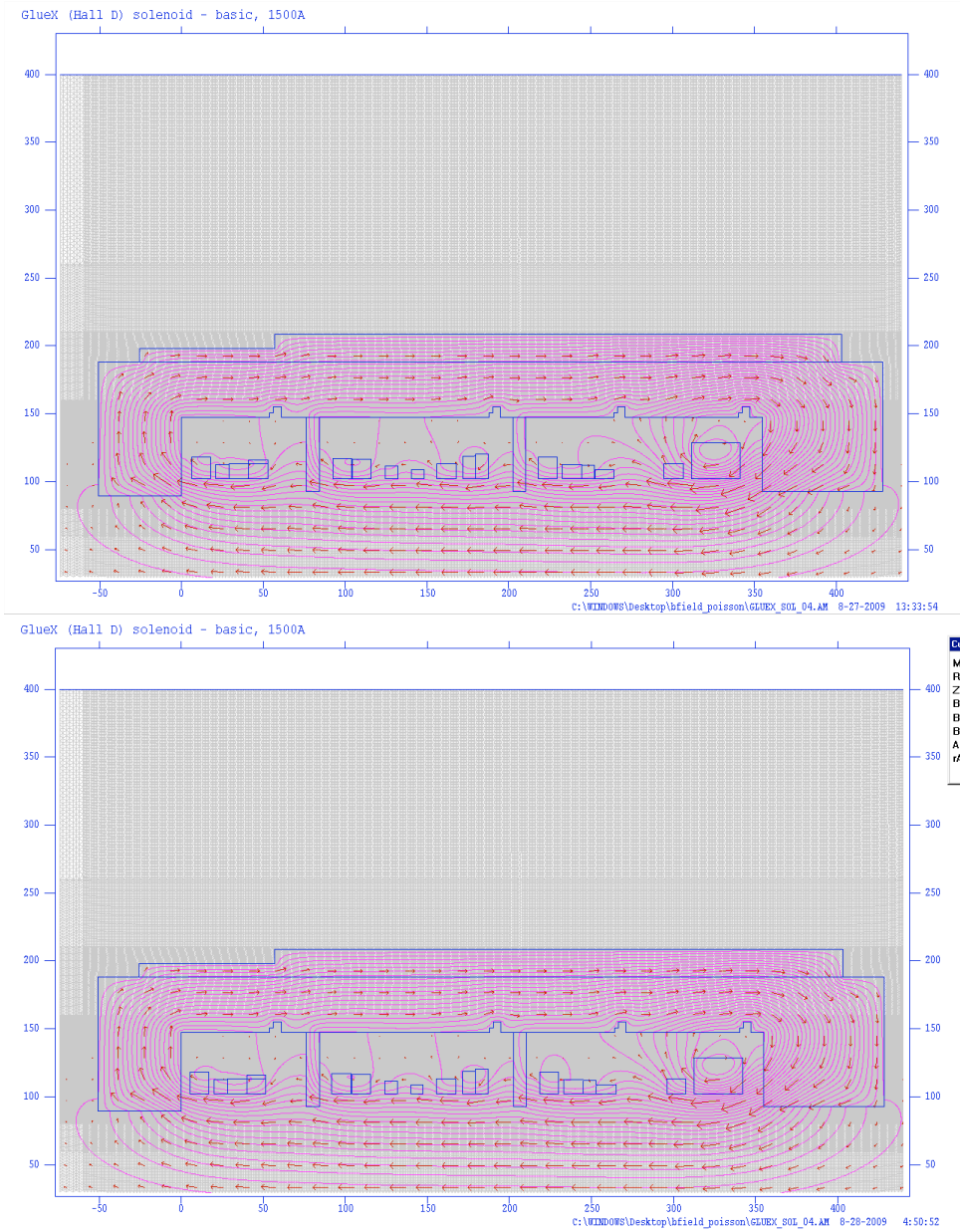


Figure 8: B-Field generated by Poisson/Superfish as draw by the wfspplot.exe program. Both plots represent geometries where the coils are shifted in z from the nominal. The upper plot is for the 20090827\_01 configuration and the lower is for the 20090827\_02 configuration (see text for details on the different configurations).

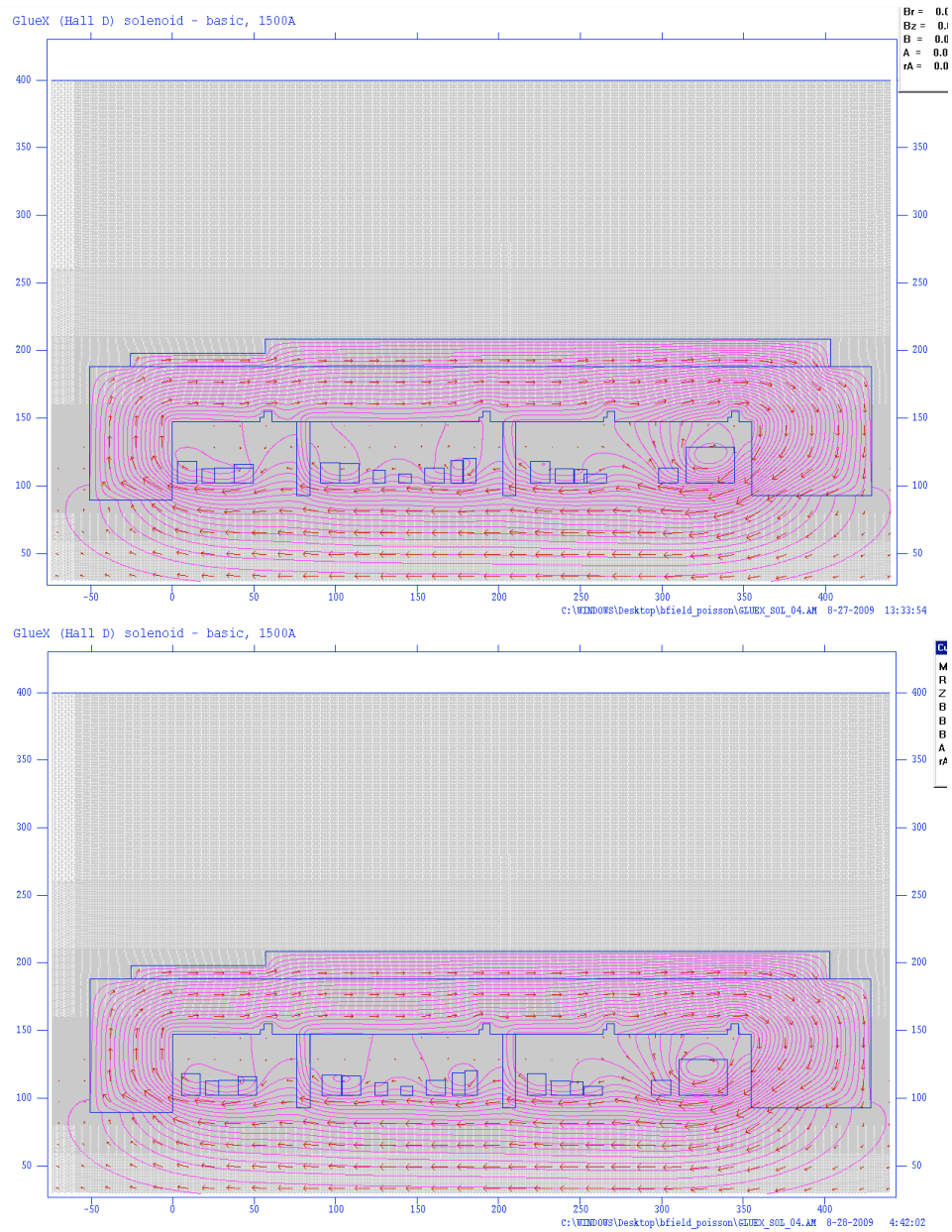


Figure 9: B-Field generated by Poisson/Superfish as draw by the wfplot.exe program. Both plots represent geometries where the coils are shifted in z from the nominal. The upper plot is for the 20090827\_03 configuration and the lower is for the 20090827\_04 configuration (see text for details on the different configurations).

Figure 12 shows plots comparing the ANSYS and POISSON maps for different slices in either R or z. Included in the plots are two POISSON generated maps where the grid spacing of the mesh different by a factor of 2 in both the R and z dimensions. Note that for all of the plots, the same interpolation routine was used to calculate the field at specific points in space. It is interesting to note the odd shape of the ANSYS generated map in the upper right plot of figure 12 as compared to the more smoothly varying POISSON generated map.

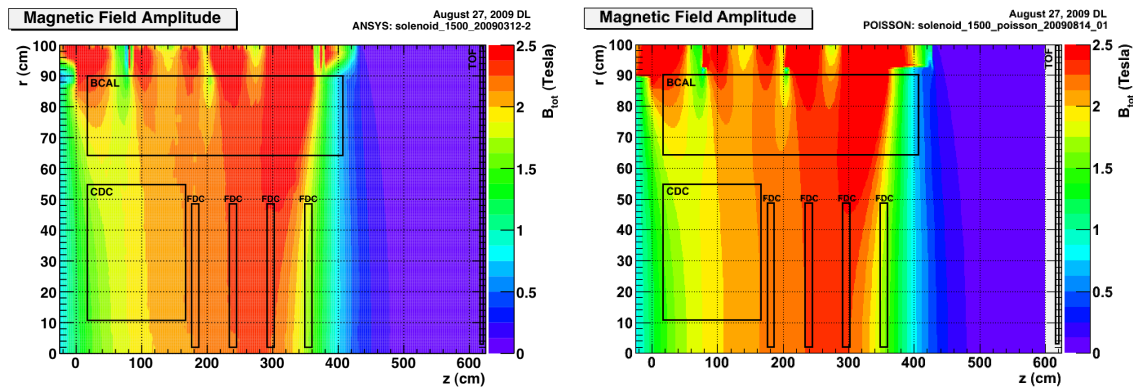


Figure 10: Magnetic field amplitude as calculated by ANSYS (left) and POISSON/Superfish (right).

Figure 13 shows the difference of the direction of the field vectors for each of the 4 shifted field maps relative to the map using the nominal coil positions. The lower left plot in the figure represents the largest coil shifts in the present study (4cm or 2cm, depending on the coil). That plot indicates that in the region of the tracking chambers, the field direction varied by only few milliradians with higher, 10-20 mrad deviations only in the outer corners of the active area. Realistically, we expect to know the coil positions to within a few millimeters making the top left plot in figure 13 the closest match to our expected uncertainty in the field.

Figure 15 shows a comparison of the magnitudes of the B-field between each of the shifted coil geometries and the the nominal geometry. Figure 15 shows a similar set of plots, but of the relative difference in percent rather than than an absolute difference.

## 4 Field Map Uncertainties

Two sets of 1000 single  $\pi^+$  track events were generated using the nominal 20090814\_01 map. One set with multiple scattering turned on and the other without. Both sets had everything else (energy loss, particle decays, secondary particle tracking, etc. ...) turned off. Figure 16 shows the FDC residuals for the case when multiple scattering is turned on.

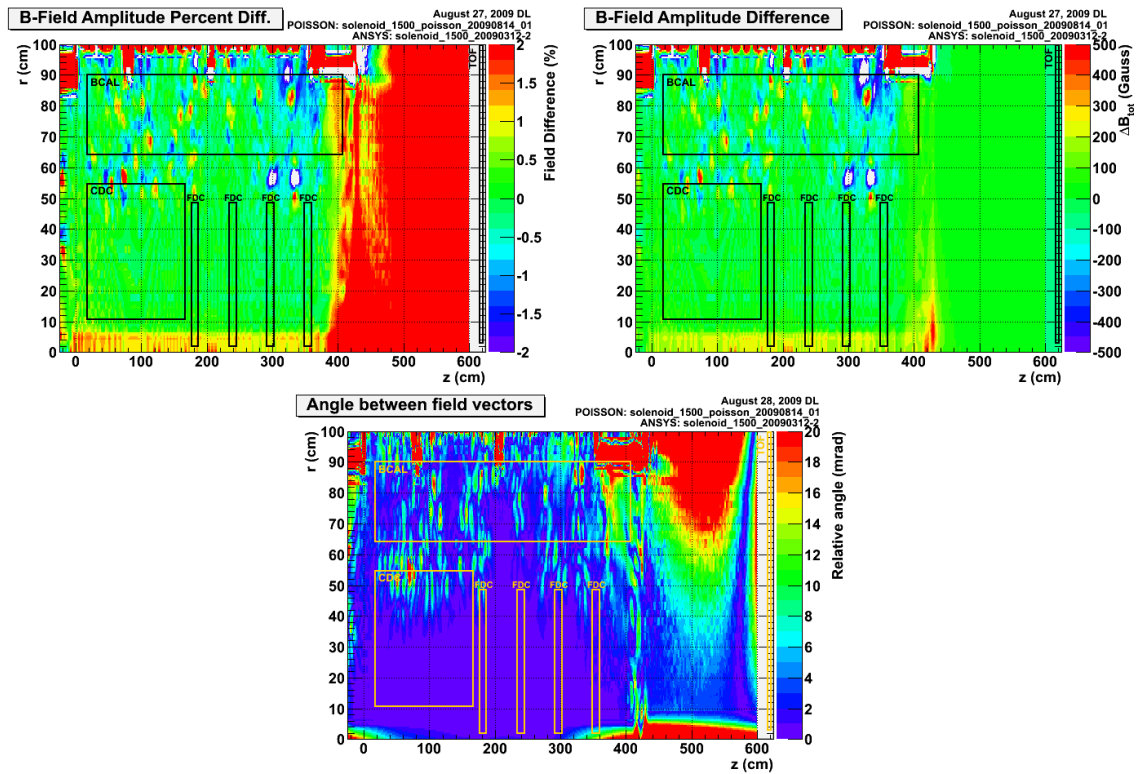


Figure 11: Comparison of field maps generated by ANSYS and POISSON. The top left plot is of the relative percentage difference of field magnitudes. The top right is the absolute difference of field magnitudes in Gauss. The bottom plot is the difference in the field directions expressed as the angle between the field vectors.

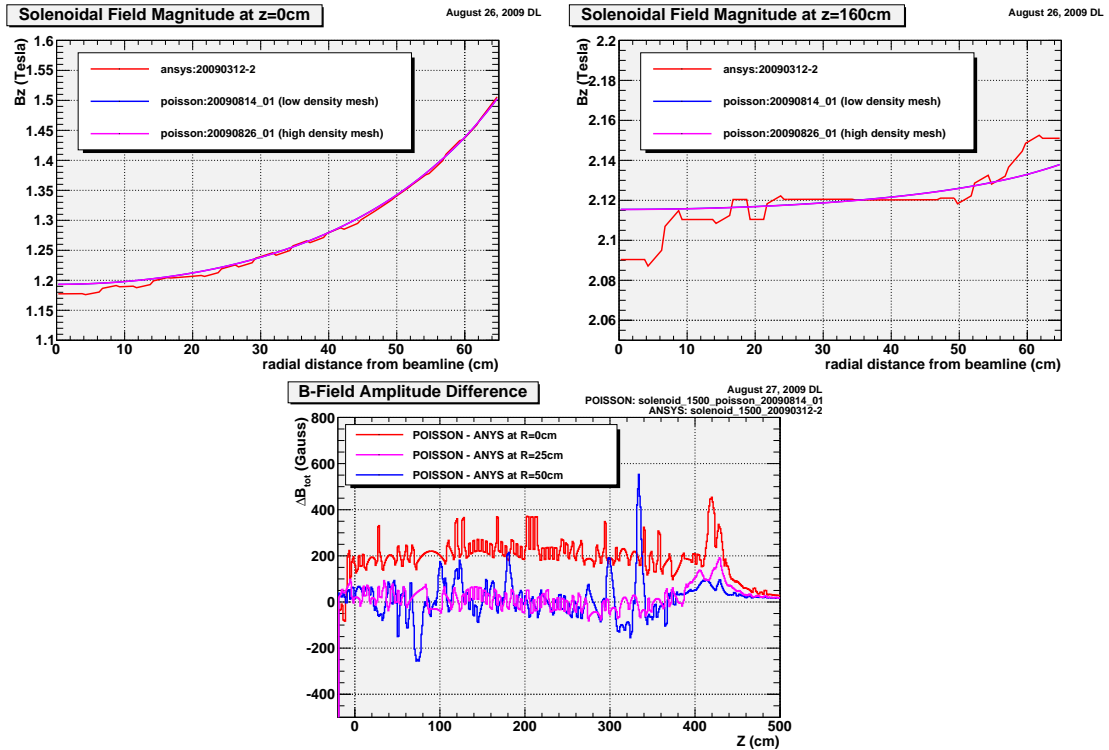


Figure 12: Comparison of field maps generated by ANSYS and POISSON. The top left shows the field magnitude at  $z=0$  as a function of  $R$ . The top right shows a similar comparison at  $z=160$ . The bottom plot shows the difference between the two maps along the beamline.

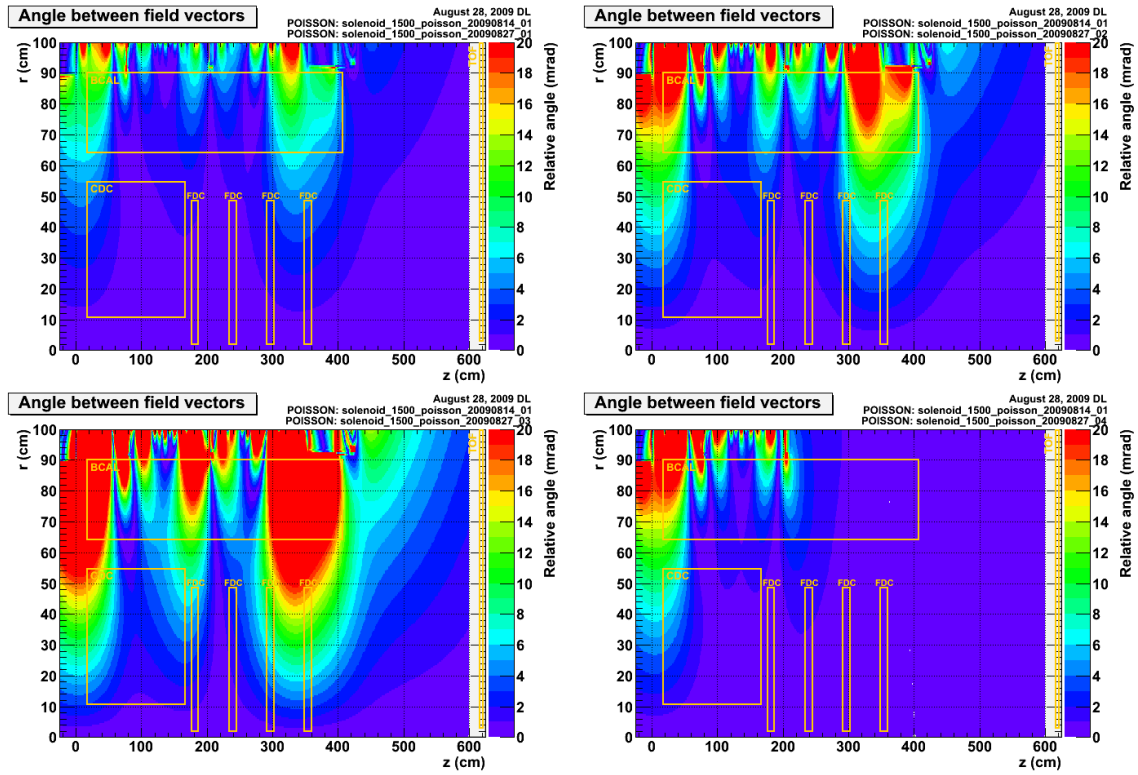


Figure 13: Comparison of B-field direction for field maps generated by POISSON with coils shifted by various amounts. The differences are all taken relative to the 20090814\_01 map. The maps are: top left=2009027\_01; top right=20090827\_02; bottom left=20090827\_03; bottom right=20090827\_04. See the text for detailed descriptions of the maps.

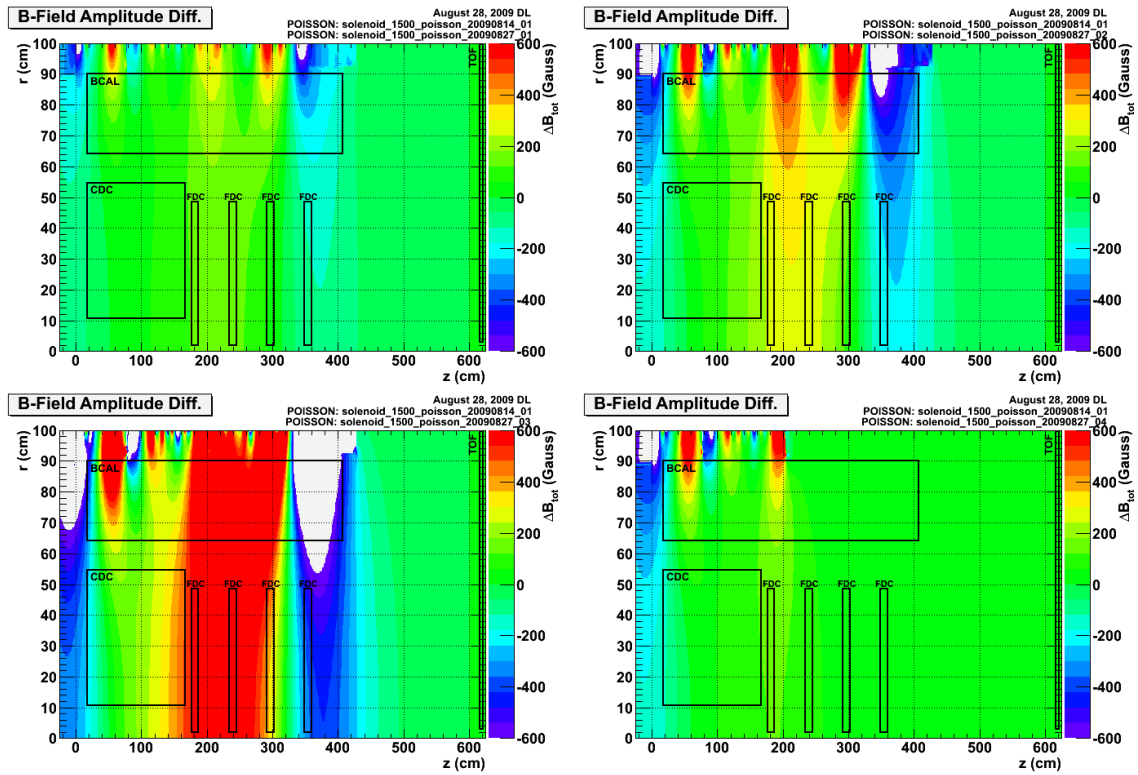


Figure 14: Comparison of B-field magnitude for field maps generated by POISSON with coils shifted by various amounts. The differences are all taken relative to the 20090814.01 map. The maps are: top left=2009027\_01; top right=20090827\_02; bottom left=20090827\_03; bottom right=20090827\_04. See the text for detailed descriptions of the maps.

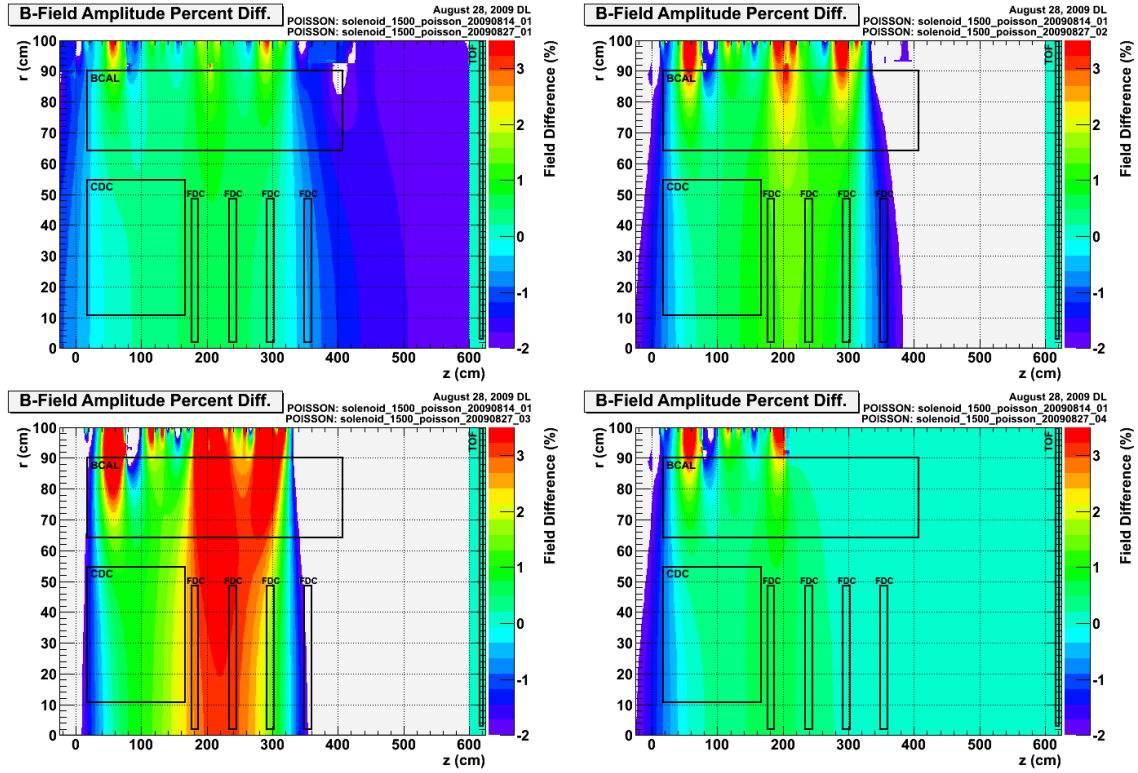


Figure 15: Comparison of relative B-field magnitude for field maps generated by POISSON with coils shifted by various amounts. These plot the difference as a percentage of the magnitude (as opposed to figure 15 which plots the absolute differences). The differences are all taken relative to the 20090814\_01 map. The maps are: top left=2009027\_01; top right=2009027\_02; bottom left=2009027\_03; bottom right=2009027\_04. See the text for detailed descriptions of the maps.

Tracks were swum using the thrown values (no fit was performed) showing the cumulative effect of the differences between the true and believed field maps. Figure 17 shows a similar plot for when multiple scattering was turned on. This figure shows how multiple scattering can dominate the residuals. However, when fitting is done (figure 18) multiple scattering in the target and start counter are effectively removed leaving only multiple scattering in the material of the chambers themselves. The two worst case situations, maps 20090827\_02 and 20090827\_03, now show that the field uncertainty now becomes comparable to multiple scattering in the chambers leading to larger residuals in FDC package 3.

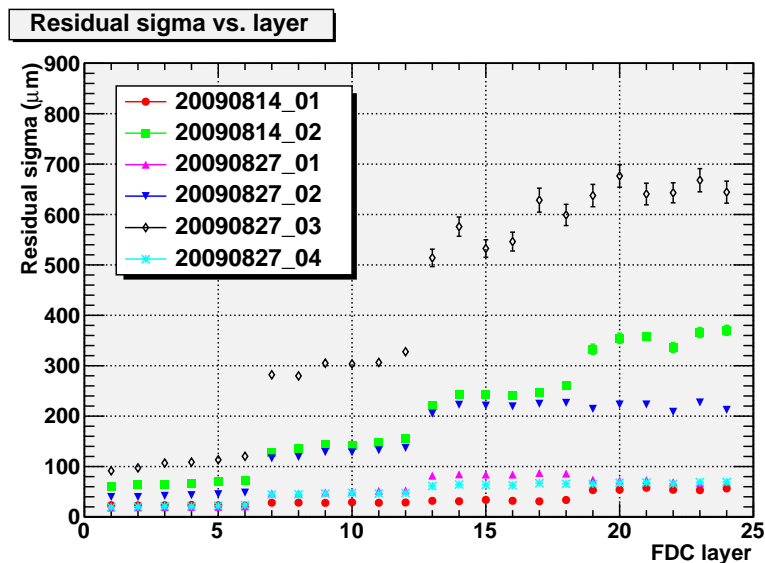


Figure 16: FDC residual for tracks swum with various magnetic field maps using hits produced when using the 20090814\_01 map. The higher FDC layer numbers correspond to layers further from the target. The tracks were generated with no multiple scattering, energy loss, or detector resolution smearing. The tracks were swum using the *thrown* parameters (not fit parameters).

A set of 10000  $\gamma p \rightarrow \rho p \rightarrow \pi^+ \pi^-$  events with an artificially narrow width ( $1 \text{ MeV}/c^2$ ) were generated using *hdgeant* and then had the drift times smeared to the nominal position resolutions using *mcsmeasr*. The smeared events were then reconstructed using each of the 4 shifted maps (figure 19) and the map generated with 1% less current (figure 20).

The upper left plot in figure 19 shows that even when reconstructing with the same field map as was used in the simulation, the mean of the  $\rho$  peak is shifted down by about 2 MeV from the thrown value of 770 MeV. This is due to a systematically low momentum reconstructed for very forward going pions (see figures 20 and 22). The only plot in figure 19 showing a significant deviation from this baseline is in the lower left corresponding to field map 20090827\_03 which had the largest coil shifts ( $\pm 4 \text{ cm}$  and  $\pm 2 \text{ cm}$ ). No differences

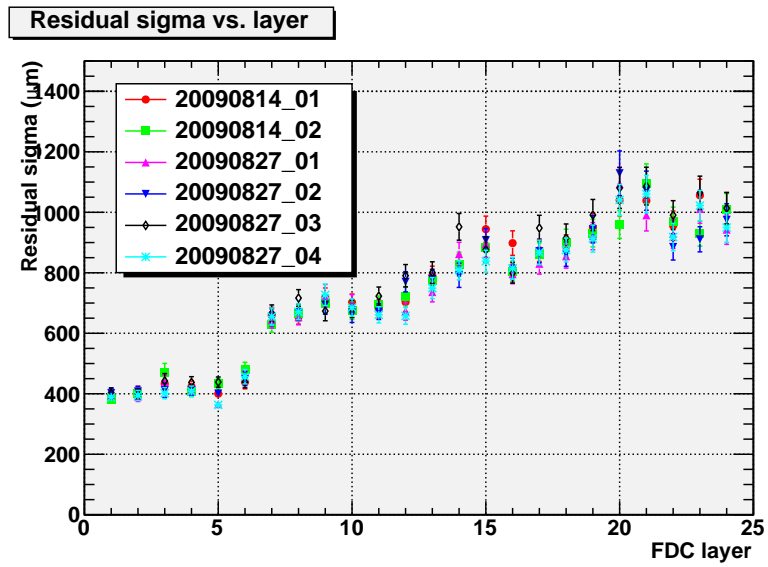


Figure 17: Similar to figure 16 except multiple scattering was included. This indicates how multiple scattering effects dominate over magnetic field uncertainties. Note that these are, again, from swimming *thrown* parameters (not fit parameters). See figure 18 for the residual distributions for fit values. The hits do not include detector resolution smearing.

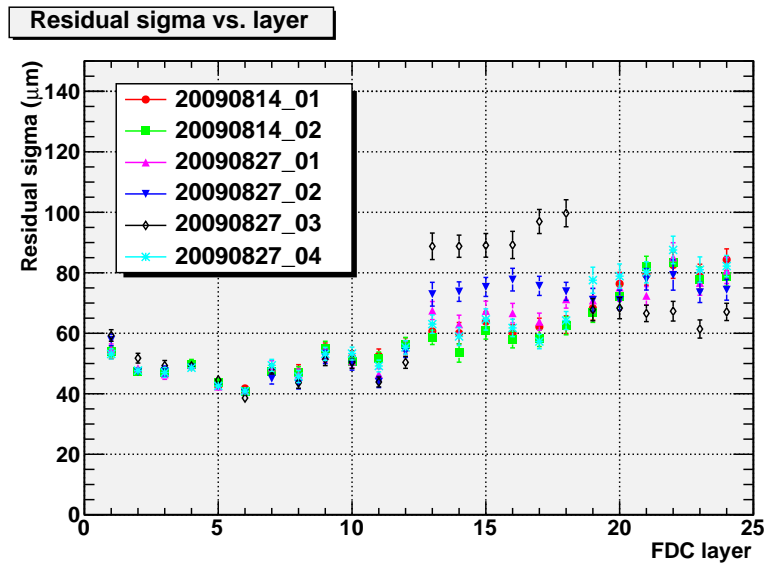


Figure 18: Similar to figure 17 except tracks were the result of fitting. Interestingly, the fit reduces the residuals to the point where the different trajectory shapes (due to the differences in the magnetic field maps) emerges in the 3rd package. The hits do not include detector resolution smearing.

in the widths of the  $\rho$  peaks is observed.

Figure 20 shows a similar pair of plots (with the one on the left being identical to the upper left plot in figure 19). The plot on the right was made using field map 20090814\_02 which had the coils in their nominal positions, but carrying 1% less current. This indicates an 8 MeV shift from nominal and a 6 MeV shift from the value achieved with no uncertainty in the field map. It is interesting to note that this deviation is even greater than the worst case seen in figure 19 even though the discrepancy between the 20090814\_01 and 20090827\_03 maps shown in figure 15 gets as high as 3% in the FDC region.

Figure 21 shows the systematic and statistical uncertainties for single  $\pi^+$  and  $\pi^-$  tracks from  $\rho$  decays. In particular, the plot on the lower right shows that even for the worst case uncertainty in the field map, there is no systematic shift in the  $4^\circ - 6^\circ$  region (where at least one high momentum track tends to go from every decay). This is the reason for the apparently better result than was achieved for the case of a 1% reduced field (figure 21). The systematically high and systematically low field in the FDC region relative to the nominal map tend to balance out leading to no systematic shift in an important region of the phase space occupied by pions in this reaction.

Figure 22 shows statistical and systematic uncertainties as a function of polar angle  $\theta$  similar to figure 21 except the shifted coil maps are replaced with the map generated with 1% reduced current. Using the map with reduced current results in a  $\sim 1\%$  systematic reduction in momentum magnitude as expected except in the region below  $4^\circ$  where there is a systematic shift that is also present when reconstructing with zero field uncertainty.

## 5 Conclusion

Reconstructed parameters appear to have uncertainties dominated by intrinsic detector resolutions and multiple scattering effects. Deviations of the magnetic field uncertainty up to 1% have no significant impact on reconstructed values. Overall systematic shifts of the magnetic field from what is expected do lead to a proportional change of reconstructed momentum (as it must). Shifting coil positions by up to 1 cm will result in less than 1% deviation in the field uncertainty. This does not consider uncertainty in the current or azimuthal asymmetry of the coils.

Based on the evidence here and the expected accuracy to which the coil positions will be known, a detailed map of the GlueX detector's solenoidal field does not appear to be warranted.

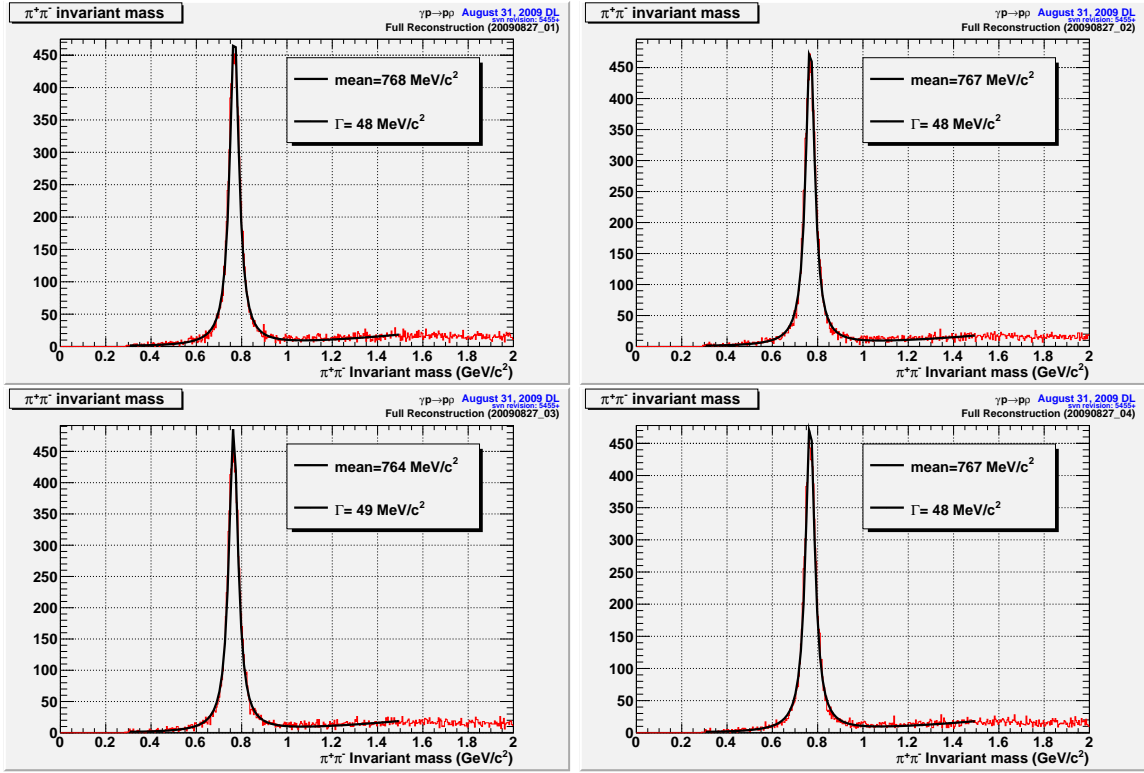


Figure 19: Similar to figure 20, but with reconstruction done using different magnetic field maps. The maps used are: top left=20090827\_01; top right=20090827\_02; bottom left=20090827\_03; bottom right=20090827\_04. See the text for detailed descriptions of the maps.

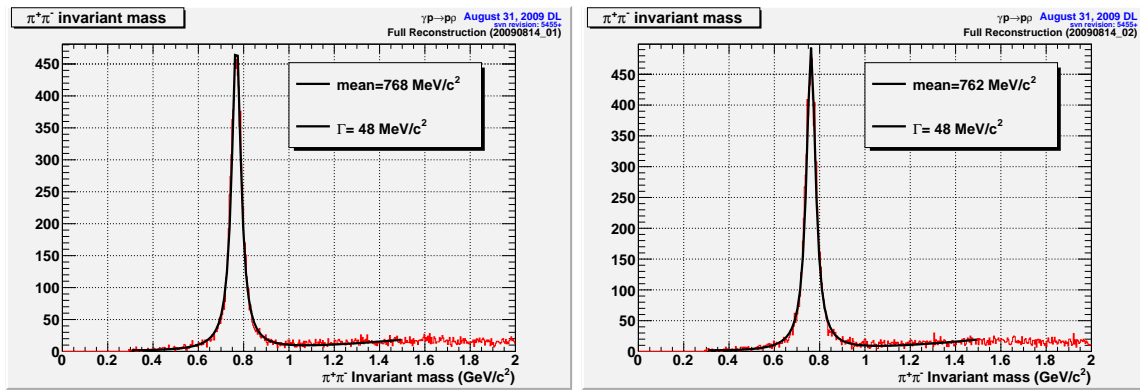


Figure 20: Fit to fully reconstructed GEANT data of  $\rho p$  events where a width of  $1\text{MeV}/c^2$  was used (instead of the actual width of  $150\text{MeV}/c^2$ ). Both plots use the same simulated data file, but the plot on the right was reconstructed using a B-field with a 1% reduction in current.

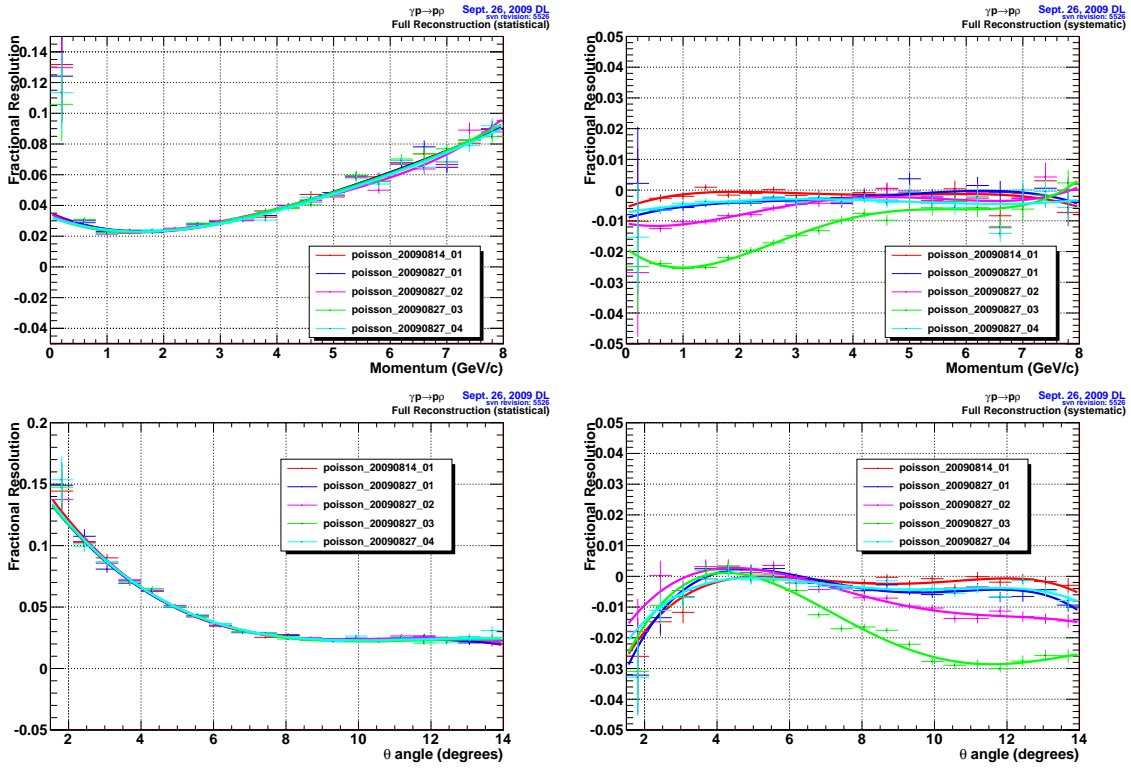


Figure 21: Plots of the statistical (left) and systematic (right) momentum uncertainties for pions in  $\gamma p \rightarrow \rho p$ . Uncertainties are plot vs momentum (top) and  $\theta$  (bottom) are shown. The curves are polynomial fits merely to help guide the eye. The green points (worst case in statistical plots) is for the case when the outer (inner) coils were shifted by 4cm (2cm).

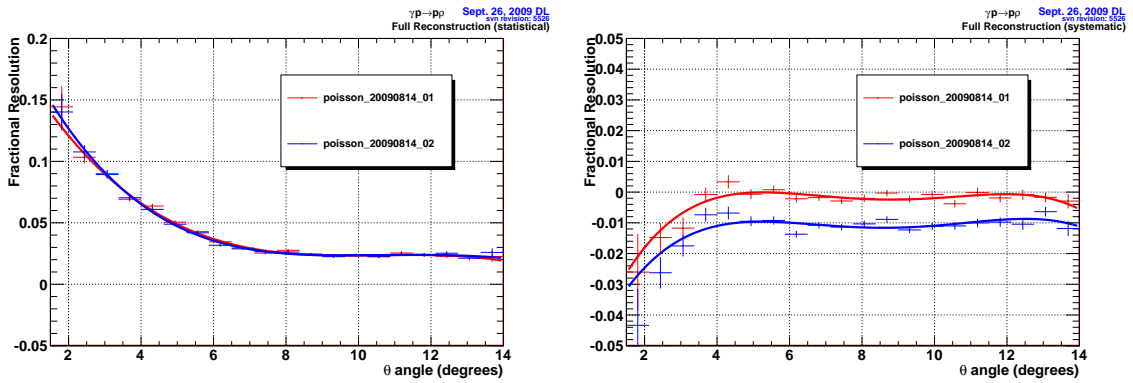


Figure 22: Plots of the statistical (left) and systematic (right) momentum uncertainties for pions in  $\gamma p \rightarrow \rho p$  using the nominal (red) map and one with 1% reduced current (blue). As expected, the blue curve shows a reduction in the reconstructed momentum of  $\sim 1\%$ .